Cytotoxic/antiproliferative effects of new [1,2,4]triazolo[4,3-c]quinazolines in tumor cell lines HeLa and B16*

S. JANTOVÁ[1], S. LETAŠIOVÁ[1], R. OVÁDEKOVÁ[2], M. MÚČKOVÁ[3]

[1]Institute of Biochemistry Nutrition and Health Protection, e-mail: sona.jantova@stuba.sk, and [2]Institute of Analytical Chemistry, Faculty of Chemical and Food Technology, Slovak University of Technology, SK-81237 Bratislava, Slovak Republic; [3]Drug Research Institute, SK-90001 Modra, Slovak Republic

Received January 16, 2006

Quinazolines – 1,3-benzodiazines are biological active compounds, and some of them act as anticancer drugs. We evaluated cytotoxic/antiproliferative activity of new synthetically prepared [1,2,4]triazolo[4,3-c]quinazolines using tumor cell lines HeLa and B16. The *in vitro* cytotoxic studies of the most active derivative 3-(5-nitro-2-thienyl)-9-chloro-5-morpholin-4-yl[1,2,4]triazolo[4,3-c]quinazoline (NTCHMTQ) were complemented by cell cycle analysis, and determination of apoptotic DNA fragmentation. Possible direct interaction of NTCHMTQ with calf thymus DNA was tested by the DNA-modified screen-printed electrode. Five quinazoline derivatives tested acted cytotoxically on both tumor cell lines. The melanoma cells B16 were more sensitive to quinazolines treatment than HeLa cells. The most effective derivative was NTCHMTQ which manifested significant *in vitro* cytotoxic/antiproliferative effect. NTCHMTQ at micromolar concetrations induced morphological changes and necrosis of B16 cells. NTCHMTQ at concentrations tested did not cause changes in cell cycle, did not induce apoptotic cell death in the B16 cells and did not even behave as a typical intercalating agent.

Key words: [1,2,4]triazolo[4,3-c]quinazolines, cytotoxic/antiproliferative effects, B16 and Hela cells, necrosis, DNA damage

Recent development in the chemistry of quinazoline derivatives gave rise to more than ten thousand publications or patents, and yielded more than one thousand derivatives. It was stimulated by the pharmaceutical utilization of some alkaloids with quinazoline skeleton, which are freely found in nature. There are four types of alkaloids, from which, e.g., febrifugine known as Chans-San,s alkaloid was used as an antimalaricum 200 years B.C. [1]. Most of these compounds were tested for their pharmacological, phytoeffective, biocide and other properties.

At present, quinazoline derivatives are used in the pharmaceutical industry, in medicine and in agriculture because of their antimicrobial [2], antiinflammatory [3], diuretic [4], anticonvulsant [5], antiallergic [6], antihypertensive [7], antiparkinsonian [8] effects and other properties.

As documented in the literature, many derivatives act as anticancer active compounds [9, 10] and they act as multitarget agents [11]. They are antifolate thymidylate synthase inhibitors [12]; epidermal growth factor receptor tyrosine kinase inhibitors [13]; inhibitors of enzymes dihydrofolate reductase [14] and tyrosine kinase [15], aldozreductase [16] and cyclic GMP phosphodiesterase [17]. Some quinazolines interact with cytoskeleton [18], they induce apoptosis [19] and influence DNA topoisomerase [20]. There are now a number of thymidylate synthase inhibitors in development (CB3717, ZD1694, LY231514, AG331, AG337). These have broad spectrum of activity against different types of human cancers. Some of these (ZD1836, ZD 6474, OSI-774, GW-2016) are now in clinical testing [13, 21].

In the aim of obtaining new antitumor agents, a series of substituted triazoloquinazolines was prepared [22, 23]. These compounds were firstly tested for antimicrobial prop-

*This study was supported by the Grant Agency for Science Research of the Ministry of education of the Slovak Republic, VEGA numbers 1/1173/04 and by Science and Technology Assistance Agency under the contract No. APVT-20-007304, APVT-20-015904 and APVT-51-019402.

erties *in vitro* on selected microorganisms [24]. The broadest antimicrobial activity was found with NTCHMTQ in concentration of 24 μM for *Bacillus subtilis*, 120 μM for *Staphylococcus aureus* and 240 μM for *Candida tropicalis*. The highest tested concentration of this derivative caused 83.1% growth inhibition of *Rhizopus nigricans*.

The main aim of this study was to investigate the cytotoxic or antiproliferative effects of synthetically prepared fifteen substituted [1,2,4]triazolo[4,3-c]quinazolines (Tab. 1) on the transformed cell line HeLa. Simultaneously, the relation between their structure and their cytotoxic effect was studied. Futher we investigated antiproliferative activity *in vitro* of the most effective derivative NTCHMTQ. Furthermore, its effect on cell morphology, cell cycle and induction of apoptosis/necrosis in murine melanoma B16 cell lines were monitored. The damage of calf thymus DNA was tested by the DNA-modified screen-printed electrode, too.

Material and methods

Cells. The human tumor cell line HeLa and murine melanoma cell line B16 (both obtained from the American Type Culture Collection (Rockville, MD, USA)) were adherently grown and propagated in minimal Eagle medium supplemented with heat-inactivated foetal bovine serum (10% (v/v) for HeLa cells and 15% (v/v) for B16 cells); penicillin/streptomycin (100 μg/ml) and kanamycin (100 μg/ml) (all obtained from Biocom Bratislava, Slovakia). To maintain exponential growth, the cultures were divided every third day by dilution to concentration of $3x10^4$ HeLa cells/ml and $8x10^4$ B16 cells/ml. Viability of the cells was determined by 0.4% trypan blue staining.

Table 1. Values IC_{50} and IC_{100}* for HeLa cells exposed for 24 h to the substituted [1,2,4]triazolo[4,3-c]quinazolines, the cell viability was measured by KB assay

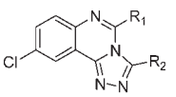

Compound	R_1	R_2	IC_{50}	IC_{100}
1	Mo	3-indolyl	10.99	247.04
2 **	Mo	5-nitro-2-thienyl	14.37	24.0
3	Mo	5-nitro-2-furyl	24.67	124.84
4	Mo	5-phenylsulfonyl-2-furyl	189.32	>201.82
5	Mo	5-acetyl-2-furyl	>251.38	>251.38
6	Mo	5-bromo-2-furyl	136.09	230.15
7	Mo	4-acetamidophenyl	>236.69	>236.69
8	Mo	2-nitrophenyl	>243.61	>243.61
9	Mo	2-chlorophenyl	>250.0	>250.0
10	Mo	4-chlorophenyl	80.25	>210.35
11	PhP	5-nitro-2-furyl	114.75	210.13
12	PhP	5-chloro-2-furyl	>214.92	>214.92
13	PhP	2-furyl	>232.13	>232.13
14	PhP	5-bromo-2-furyl	>196.16	>196.16
15	PhP	4-(N,N-dimethylamino-phenyl)	>206.61	>206.61

*Such concentration of derivatives which, in comparison to the control, inhibited the contents of proteins by 50 and 100%, values are in μM and were read out from the toxicity curves; **compound 2 = NTCHMTQ; Mo – morpholine, PhP – N-phenylpiperazine. Data represent means ±SD of three independent experiments. SD is <10%.

Cell treatment. Exponentially growing cells (24 h) in cultivation dishes at concentration of $3x10^4$ HeLa cells/ml and $1x10^5$ B16 cells ml were immediately treated with tested triazoloquinazolines at concentrations in the range of 251.4–0.251 μM for Kenacid blue (KB) assay; 240–2.4 x 10^{-4} μM for the growth inhibition assay and morphological observation**;** 1.2–2.4 x 10^{-2} μM for cell cycle analysis and determination of apoptosis and 240–2.4 x 10^{-3} μM for determination of mutagenic effects. DMSO (0.1%) was used as control.

Chemicals. Substituted [1,2,4]triazolo[4,3-c]quinazolines (Tab. 1) were prepared by ŠPIRKOVÁ et al [22, 23]. Chromatographically pure fifteen substituted [1,2,4]triazolo[4,3-c]quinazolines were dissolved directly in dimethyl sulfoxide (DMSO); its final concentration never exceeded 0.1% (v/v) in either control or treated samples. The solutions of tested quinazoline derivatives were prepared freshly before each incubation. Other chemicals were obtained from Sigma St Louis, MO, USA.

Kenacid blue (KB) assay. After 24 hours exposure of HeLa cells with the tested quinazolines, the wells were washed with PBS and 100 μl of the fixate-destain solution (1% acetic acid, 50% ethanol, 49% distilled water) was added. The microplates were placed on a shaker for 20 min. After removing the fixate, 100 μl of Kenacid blue R staining solution (4 mg/ml) per well was added and the multiwell plates were shaken for another 10 min. They were subsequently washed twice with PBS, 150 μl of desorbing solution (98.15 g potassium acetate, 700 ml ethanol, 300 ml distilled water) was added, and the absorbance of each well was measured. In all three cases, the 96-well plates were scanned with a HUMAREADER microplate spectrophotometer equipped with a 568 nm filter to record absorbancy. The results were calculated for each concentration as a percentage of control.

Relative inhibition was calculated using the formula:

$$\% \text{ inhibition} = 100 - \frac{A - A_x}{A - A_0} \cdot 100$$

where A_0 is absorbance A586 at the time of the addition of the respective compound; A is absorbance A_{586} of control cells, A_x is absorbance A_{586} of treated cells.

The growth inhibition assay. After 24, 48 and 72 h, the treated and control HeLa and B16 cells were washed once with phosphate buffered saline (PBS) to remove fragments and dead cells. The dishes were harvested in triplicate with 0.25% trypsin, washed once with PBS and resuspended in the latter. The cells were recognized by their ability to exclude trypan blue stain (0.4%). Unstained cells were counted in a counting chamber.

Cytotoxic effects were evaluated in terms of inhibition of

cell proliferation. Relative inhibition was calculated using the formula:

$$\% \text{ inhibition} = 100 - \frac{K - E_x}{K - K_0} \cdot 100$$

where K_0 is cell count at the time of the addition of the respective compound; K is cell count of control cells, E_x is cell count of treated cells.

Preparation for light microscopy. The suspension of the HeLa and B16 cells was prepared from 3-day culture at a cell density of $3x10^4$ HeLa cells/ml and $8x10^4$ B16 cells/ml. Sterile micro-cover slips (15x15x1 mm) were placed on the bottom of plastic dishes (∅60 mm). These cover slips were treated with 0.5 ml of the above-mentioned suspension. After 30 minutes, 4.5 ml of culture medium was added to the dishes and the cells were cultured for 24 h at 37 °C in a humidified atmosphere containing 5% CO_2. Then the tested quinazoline (NTCHMTQ) was added to the cells and after 24, 48 and 72 h of treatment the cover slips with adhering control and treated cells were taken out of the culture medium and photographed under a light microscope (Meopta).

Flow cytometric analysis of cell cycle. Flow cytometry was performed by using Epics XL flow cytometer (A Beckman Coulter Company, USA) equipped with an argon laser operating at 488 nm for excitation of the propidium iodide. The B16 cells ($0.5x10^6$) treated with 1.2; 0.24 and 0.12 μM were exposed to 0.1% Triton X-100 in PBS supplemented with RNA-ase (50 μg/ml) for 25 min at 37 °C. Afterwards, DNA was stained by propidium iodide (50 μg/ml) for 15 min at 4 °C. Samples were analyzed by EPICS XL with the use of software System II provided by the manufacturer.

Detection of damage to DNA by using screen-printed electrode [25]. For voltammetric measurements, a computerized voltammetric analyzer ECA pol, model 110 (Istran, Bratislava, Slovakia) fitted with a screen-printed three-electrode assembly (FACH, Presov, Slovakia) including a carbon working electrode (SPE, 25 mm^2 geometric surface area), a silver/silver chloride reference electrode (Ag/AgCl/SPE with the potential of 0.284 V vs conventional Ag/AgCl/sat. KCl electrode) and a carbon counter electrode was used for voltammetric measurements. The working electrode without any electrochemical preconditioning was chemically modified *ex situ* by covering with 5 μl of the DNA solution (0.1 mg/ml) and leaving the electrode to dry overnight. The measurements were carried out in a 10 ml glass one-compartment voltammetric cell at room temperature (22 °C) and visible light.

DNA marker signal. The modified procedure reported previously was used for the measurement with the DNA redox marker. Briefly, the DNA/SPE sensor was pre-treated by immersing to $5x10^{-3}$ M phosphate buffer pH 7.0 under stirring for 5 min, and then rinsed with water. The $[Co(phen)_3]^{3+}$ marker was accumulated from 5 ml of its $5x10^{-7}$ M solution in $5x10^{-3}$ M phosphate buffer under stirring for 120 s at an open circuit. The differential pulse voltammogram (DPV) was recorded immediately from +0.300 to –0.500 V at the pulse amplitude of 100 mV, the scan step of 5 mV and the scan rate of 10 mV/s. The DNA marker peak current was obtained using the evaluation against a base-line by standard software and the subtraction of the mean marker peak current measured at the unmodified SPE (n=10) under the same conditions. Then, the DNA/SPE sensor was regenerated by a removal of the electrostatically accumulated $[Co(phen)_3]^{3+}$ ions from the DNA layer at treating in the buffer medium of higher ionic strength ($1x10^{-1}$ M phosphate buffer pH 7.0) under stirring for 60 s. A negligible marker signal was checked by the DPV record in blank. The marker peak current was obtained in triplicate and its mean value was calculated (I_0). To detect the damage to DNA, the same DNA/SPE sensor was incubated in quinazoline solution (240, 120, 24, 2.4, 0.24 μM) in $5x10^{-3}$ M phosphate buffer pH 7.0 for 10 min under stirring, and then rinsed with water. The DNA marker peak current was obtained in duplicate after medium exchange for $5x10^{-7}$ M $[Co(phen)_3]^{3+}$ in $5x10^{-3}$ M phosphate buffer using the DPV measurement/biosensor regeneration scheme (see above) and the mean value was calculated (I). Finally the normalized (relative) signal I/I_0 was received.

Signals of DNA bases. The anodic signals of 8-oxoguanine, guanine and adenine moieties were obtained at DNA/SPE in the blank $5x10^{-3}$ M phosphate buffer solution pH 7.0 recording the DPV scans from 0.1 to 1.6 V at the pulse amplitude of 100 mV, the scan step of 1 mV and the scan rate of 10 mV/s. The peak current values were evaluated against a base-line.

Statistics. All data represent the results obtained from three separate experiments (for each concentration of tested compounds five separate Petri dishes or three separate microplates were used). The individual data points are presented as the arithmetic means ±SD (standard deviation). The statistical significance of the results obtained from *in vitro* studies was evaluated by Student's t-test, with probability values of 0.05 being considered as significant.

All statistical analyses were performed in Graphic program ORIGIN 6.1, MS Excel 2003 for Windows XP.

Results

The results in the primary screening of cytotoxicity of the fifteen substituted [1,2,4]triazolo[4,3-c]quinazolines are shown in Table 1. The values of inhibitory concentrations IC_{50} and IC_{100} were obtained from the total cell protein content measured by KB assay. The highest cytotoxic effect on the HeLa cells was induced 3-(5-nitro-2-thienyl)-9-chloro-5-morpholin-4-yl[1,2,4]triazolo[4, 3-c]quinazoline (NTCHMTQ, derivative 2, IC_{50}=14.37 μM, IC_{100}=23.97 μM) and 3-(5-nitro-2-furyl)-9-chloro-5-morpholine-4-yl[1,2,4]triazolo [4,3-c]quinazoline (derivative 3, IC_{50}=24.67 μM, IC_{100}= 124.84 μM). Certain cytotoxicity was observed in 3-(3-indolyl)-9-chloro-5-morpholine-4-yl[1,2,4]triazolo[4,3-c]quinazoline (derivative 1, IC_{50}=10.99 μM, IC_{100}=247.04 μM),

Table 2. Values IC_{50} and IC_{100}* for HeLa and B16 cells exposed for 24, 48 and 72 h to the active [1,2,4]triazolo[4,3-c]quinazolines (compounds 1, 2, 3, 6, 1)

Cells	HeLa						B16					
Time (h)	24		48		72		24		48		72	
Compound	IC_{50}	IC_{100}	IC_{50}	IC_{100}	IC_{50}	IC_{100}	IC_{50}	IC_{100}	IC_{50}	IC_{100}	IC_{50}	IC_{100}
1	6.52	123.52	1.58	123.52	6.74	123.52	$0.2x10^{-1}$	24.7	$0.3x10^{-3}$	2.47	$0.3x10^{-3}$	2.47
2**	8.85	24.0	13.99	24.0	6.43	24.0	$0.2x10^{-1}$	2.41	$0.3x10^{-3}$	0.24	$0.3x10^{-3}$	0.24
3	9.01	24.97	9.66	24.97	7.79	24.97	0.12	24.97	0.7	2.49	0.7	2.49
6	5.51	115.07	4.92	170.82	0.53	115.07	2.60	23.01	$0.9x10^{-2}$	2.3	$0.9x10^{-2}$	2.3
11	–	210.12	–	210.12	–	210.12	0.41	21.01	$0.8x10^{-2}$	21.01	$0.2x10^{-1}$	21.01

*Such concentration of derivatives which, in comparison to the control, inhibited the cell number by 50 and 100%, values are in μM and were read out from the toxicity curves; **compound 2 = NTCHMTQ; Data represent means ±SD of three independent experiments. SD is <10%.

3-(5-bromo-2-furyl-9-chloro-5-morpholine-4-yl[1,2,4] triazolo[4,3-c]quinazoline (derivative 6, IC_{50}=136.09 μM, IC_{100}=230.15 μM) and 3-(5-nitro-2-furyl)-9-chloro-5-morpholine-4-yl[1,2,4]triazolo[4,3-c]quinazoline (derivative 11, IC_{50}=114.75 μM, IC_{100}=210.13 μM). Other tested [1,2,4]triazolo[4,3-c]quinazolines (derivatives 4, 5, 7, 8, 9, 10, 12, 13, 14, 15) showed weak activity (the values IC_{100} were higher than of the highest concentration tested).

Table 2 shows the values of growth inhibitory concentrations IC_{100} of five the most active derivatives (1, 2, 3, 6, 11). The values were obtained from the growth curve of HeLa and B16 cells. The most effective quinazoline on the both tumor cell lines was 3-(5-nitro-2-thienyl)-9-chloro-5-morpholin-4-yl[1,2,4]triazolo[4,3-c]quinazoline (NTCHMTQ, derivative 2).

Figure 1 represents the growth curves of HeLa cells (Fig. 1a) and B16 cells (Fig. 1b) treated for up to 72 h with NTCHMTQ at concentrations ranging from 240 to 0.24 μM for HeLa cells and from 240 to $2.4x10^{-4}$ μM for B16 cells. After 24 h, the three highest concentrations tested (240, 180 and 120 μM) had an acute cytolytic effect manifested by degeneration-lysis (necrosis) of certain parts of the HeLa cells. In the next time intervals the degeneration of cell population increased. The concentration of 24 μM induced a delayed cytotoxic effect. After 24 h of cultivation, 39.1% of the cell population proliferated but after 48 h and 72 h 100% degeneration of cell population was found. The concentration 2.4 μM of NTCHMTQ induced a cytotoxicity that was directly time-dependent. The HeLa cells treated for 72 h with the lowest concentration (0.24 μM) grew as well as the control cells. The six highest concentrations tested of NTCHMTQ (240, 180, 120, 24, 2.4, 0.24 μM) induced an acute cytotoxic effect demonstrated by degeneration of certain parts of the B16 cells (NTCHMTQ concentrations of

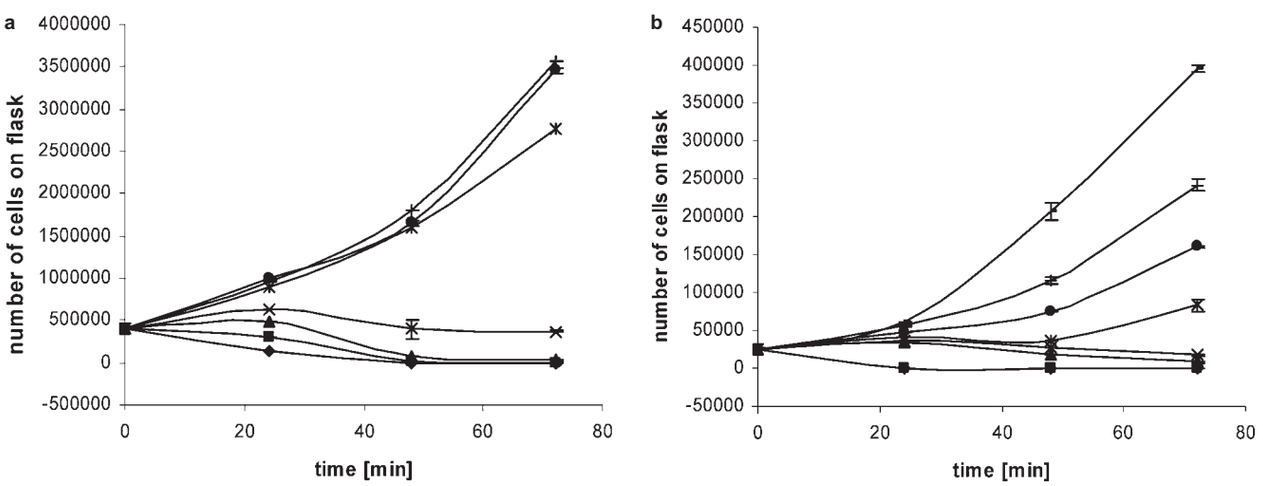

Figure 1. The growth curves of HeLa (a) and B16 (b) cells treated for up to 72 h with NTCHMTQ. Concentration of derivative (μM): (a) – for HeLa cells: + = control, ♦ = 240, ■ = 180, ▲ = 120, × = 24, * = 2.4, ● = 0.24; (b) – for B16 cells: —— = control, ♦ = 240, 180, 120, ■ = 24, ▲ = 2.4, × = 0.24, * = $2.4x10^{-2}$, ● = $2.4x10^{-3}$ and $2.4x10^{-4}$. Data represents means ±SD of three independent experiments. SD is <10%.

240, 180, 120 and 24 μM) or total inhibition of B16 cell proliferation (NTCHMTQ concentrations of 2.4 and 0.24 μM). After 24 h and 48 h of cultivation, the B16 cells treated by NTCHMTQ concentration of $2.4x10^{-2}$ μM did not proliferate, but in the next 24 h interval, 5.8% cell proliferation was found. The other two concentrations ($2.4x10^{-3}$ and $2.4x10^{-4}$ μM) manifested a cytotoxicity that was directly time- and concentration-dependent. These changes in viable cell number were also observed when aliquots of the cultures were examined by light microscopy (Figs. 2, 3).

The cytolytic effect of 3-(5-nitro-2-thienyl)-9-chloro-5-morpholin-4-yl[1,2,4]triazolo[4,3-c]quinazoline (NTCHMTQ) observed by light microscopy at concentrations 240, 180, 120 μM for HeLa cells and 24, 2.4, 0.24 μM for B16 cells during 72 h of culturing is illustrated in Figure 2 and 3. The control cells (Figs. 2a, 3a) grew on the surface of cultivation slide and during 72 h of incubating a monolayer was formed. Figures 2 b,c,d and 3 b,c,d show significant changes in morphology which occurred within 72 h in different stages of dying cell detached from the covering slip. As seen from figures NTCHMTQ induces integrity damage of cytoplasmic membrane and lysis-necrosis of cells. The dying cells were stained by trypan blue dye (0.4%).

To elucidate in more details how NTCHMTQ-treated cells are dying, we monitored cell cycle profile (Fig. 4) and induction of apoptosis (data not shown) of NTCHMTQ-treated B16 cells. As shown in Figure 4, quinazoline at concentrations of 1.2, 0.24, 0.12 and 2.4×10^{-2} μM had no effect on cell cycle profile of B16 cells. Similarly, NTCHMTQ at tested concentrations (1.2, 0.24, 0.12 and 2×10^{-2} μM) did not induce the apoptotic DNA fragmentation in B16 cells.

Damage to dsDNA was expressed by the relative signal I/I_0. dsDNA on the surface of screen-printed electrode was exposed to different concentrations (240, 120, 24, 2.4, 0.24 μM) of NTCHMTQ. Values of the relative signal of the DNA marker obtained after the biosensor incubation are summarized in Table 3. These data demonstrate practically no damage to DNA. Small damage was detected for concentration 240 μM of quinazoline. DNA marker signal was

Table 3. Effect of NTCHMTQ on dsDNA expressed by the relative DNA marker signal

Conc. of NTCHMTQ, μM	DNA marker signal (I/Io) at DNA/SPE incubated	Damage to dsDNA, %
240	0.91 ± 0.02	9
120	0.97 ± 0.03	3
24	0.99 ± 0.04	1
2.4	1.02 ± 0.04	0
0.24	1.03 ± 0.03	0

The reference I/I_0 value for 1.8 mg/l cisPt was 0.54±0.04.

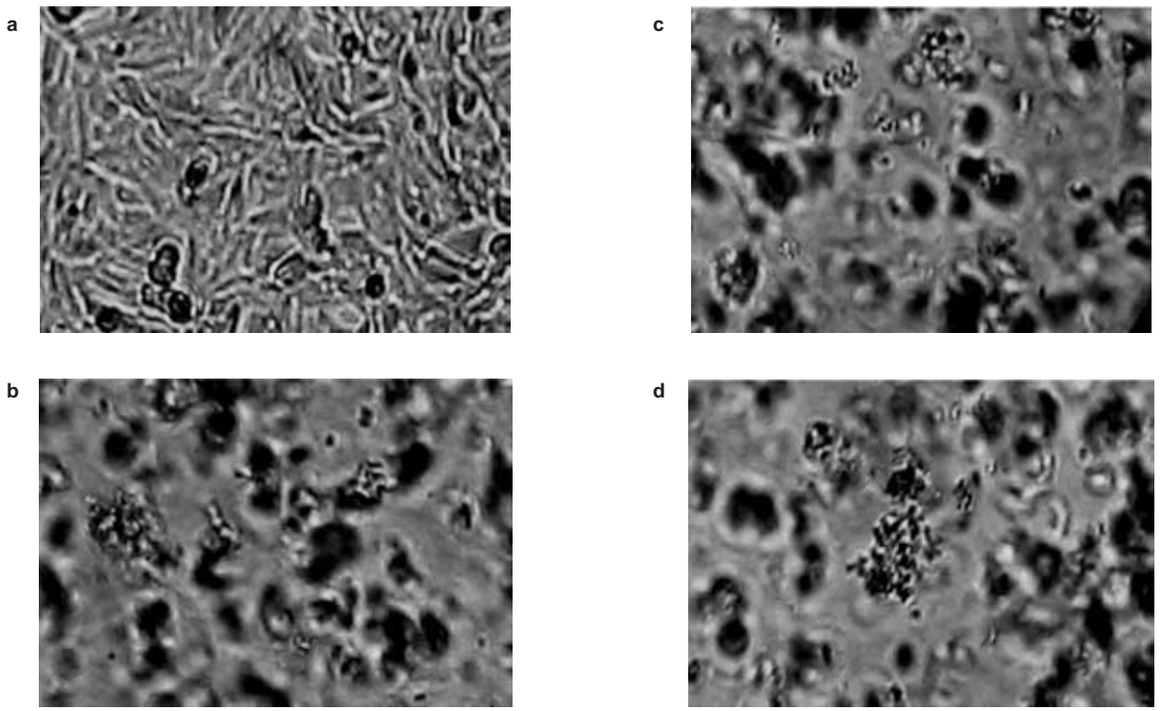

Figure 2. The cytolytic effect of NTCHMTQ on morphology of HeLa cells after 72 h exposure. Concentration of derivative (μM): a – control cells, b – 240, c – 180, d – 120. Magnification 10x8.

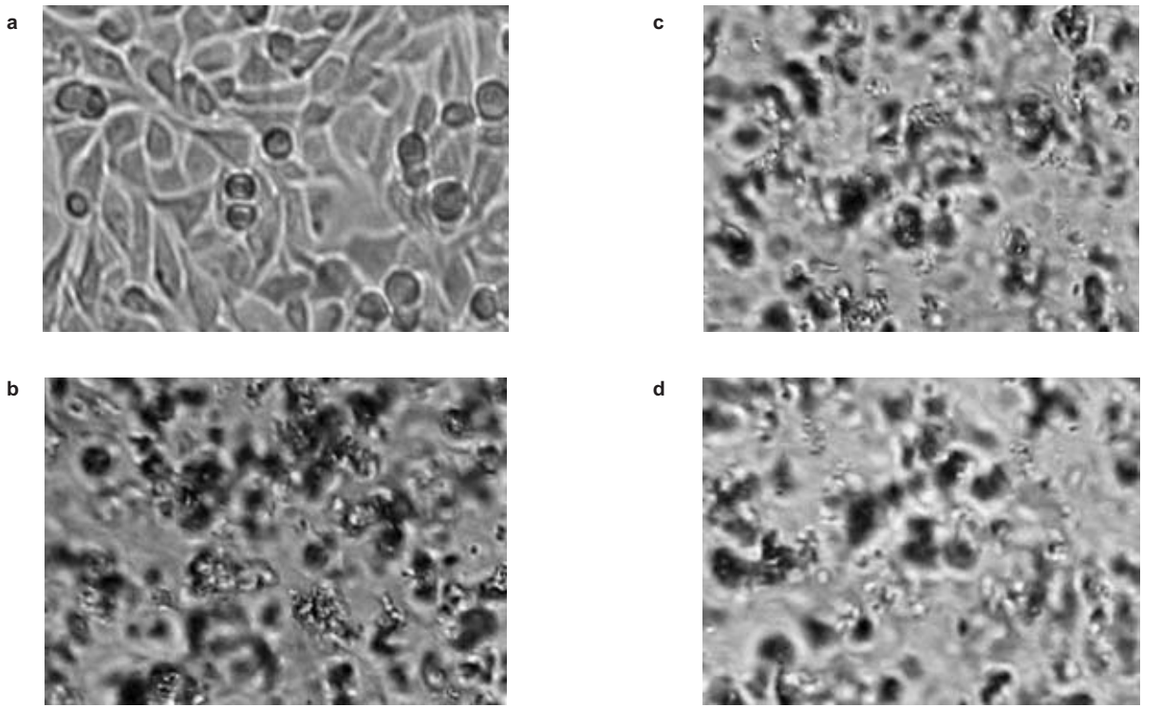

Figure 3. The cytolytic effect of NTCHMTQ on morphology of B16 cells after 72 h exposure. Concentration of derivative (μM): a – control cells, b – 24, c – 2.4, d – 0.24. Magnification 10x8.

0.91±0.02 (only 9% of damage). The reference of the relative signal I/I_0 for 1.8 mg/l cisplatin (cisPt) was 0.54±0.04.

Damage to dsDNA has also been proved by a change of voltammetric signals of the DNA bases. The incubation of DNA/SPE in the quinazoline solution for 10 min leads to no significant decrease of the anodic peaks corresponding to guanine moiety (about 700 mV) and adenine moiety (1100 mV) [26].

Discussion

With the aim of obtaining new antitumor agents, a series of substituted [1,2,4]triazolo[4,3-c]quinazolines were prepared [22, 23]. Therefore, a lot of clinically used cytostatics show antimicrobial effects too. As a first step, we tested these compounds for cytotoxic properties *in vitro* on four bacterial strains, four yeast strains and two filamentous fungi strains [17]. The most effective derivatives had the triazoloquinazoline skeleton substituted with the pharmacologically active chromophores-morpholine, chlorine and nitro-group. The broadest antimicrobial activity was found with 3-(5-nitro-2-thienyl)-9-chloro-5-morpholin-4-yl[1,2,4]triazolo [4, 3-c]quinazoline (NTCHMTQ).

Further, in our primary screening we studied cytotoxic effect of fifteen substituted [1,2,4]triazolo[4,3-c]quinazolines on human tumor cell line HeLa (Tab. 1). The highest cytotoxic effect was demonstrated by 3-(5-nitro-2-tienyl)-9-chloro-5-morpholine-4-yl[1,2,4]triazolo[4, 3-c]quinazoline (NTCHMTQ, derivative 2). The comparison of the triazole structure and it's cytotoxic effect on the HeLa cells (Tab. 1) showed that the most active derivatives were non-substituted in the aromatic ring or substituted by bromo- or chloro-group, and in the pyrimidine ring of quinazoline skeleton by phenylpiperazinyl or morpholino group. We obtained the similar results with selected microorganism.

Similarly, the quinazoline derivatives non-substituted in the aromatic ring or substituted by halogen and in the pyrimidine ring of quinazoline skeleton by phenyl or morpholino group demonstrated the most active by the study of cytotoxic effects of some substituted tetrazolo[1,5-c]quinazolines [27].

As it follows from the growth curves of the HeLa and B16 cells (Fig. 1), NTCHMTQ caused different cytotoxic effects depending on concentration and time of influence. The highest tested concentrations of quinazoline induced an acute cytotoxic effect which was manifested by immediate decrease of viable cells, respectively by the total inhibition of the cell proliferation. NTCHMTQ at concentrations of 24 μM (for HeLa cells) and 0.24 μM (for B16 cells) induced a delayed cytotoxic effect. While after the first 24 h of influence we monitored the increased cell number, in the next time intervals the decrease of cell number was found. The cytotoxic effect of NTCHMTQ at the other tested concentra-

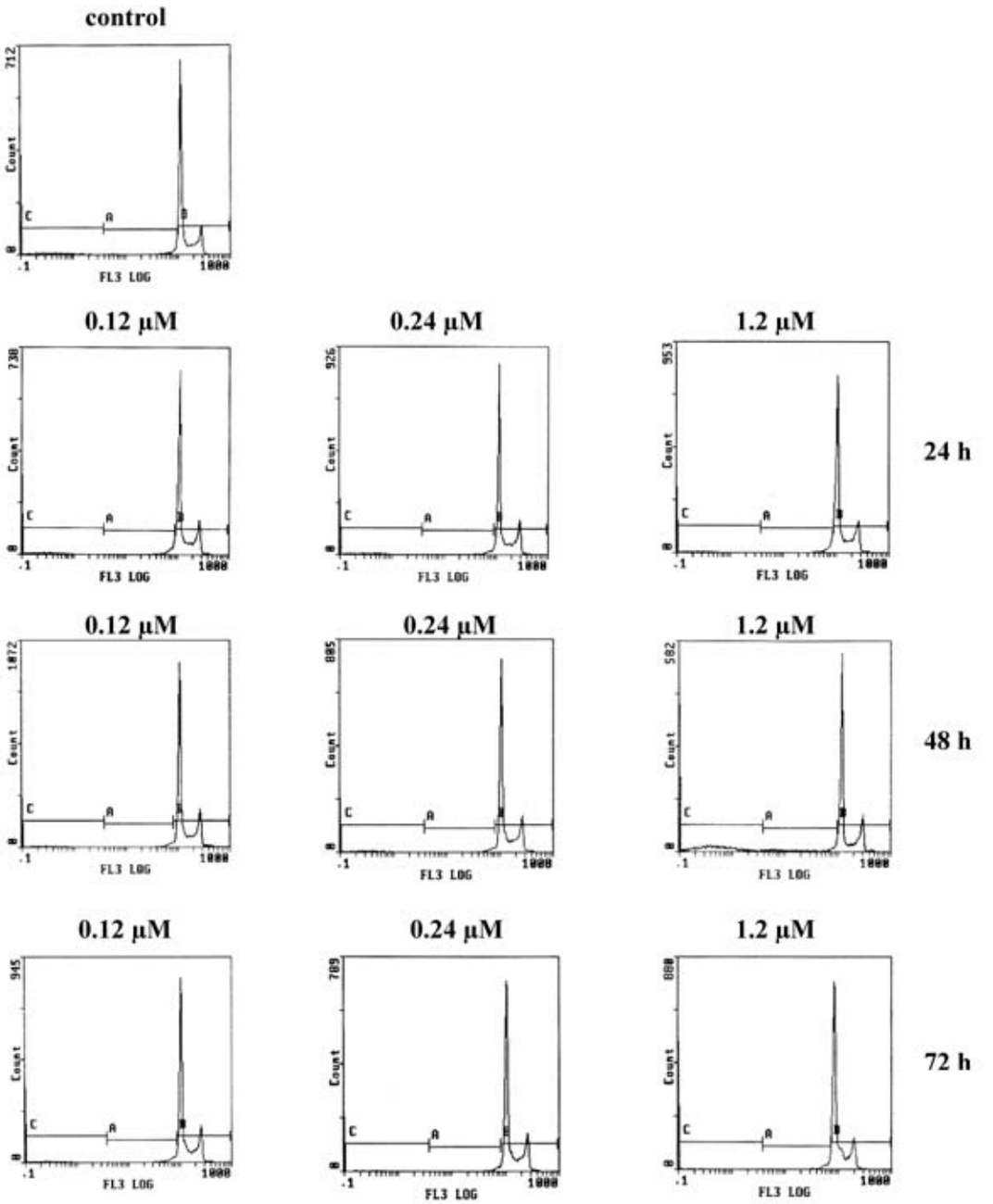

Figure 4. Flow-cytometric analysis of the untreated (control) and NTCHMTQ-treated B16 cells at concentrations of 0.12, 0.24 and 1.2 µM for 24, 48 and 72 h. A – apoptotic cells, B – intact cells, C – dead cells.

tions (2.4 µM for HeLa cells and $2.4x10^{-3}$ and $2.4x10^{-4}$ µM for B16 cells) was directly proportional to the concentration and time of influence. We observed similar type of combined cytotoxic effect by monitoring the effects of berberine on proliferation of the Hela and L1210 cells [28].

The compared values IC_{100} as determined by the cell growth inhibition assay (Tab. 2) show that the most effective quinazoline on both tumor cell lines was NTCHMTQ. The melanoma B16 cells were more sensitive to quinazolines treatment than HeLa cells.

Light microscopy (Figs. 2, 3) showed that NTCHMTQ concentration of 240, 180 and 120 µM (for HeLa cells) and

24, 2.4, 0.24 μM (for B16 cells) induced necrosis of cells (established by trypan blue).

On the basis of the results obtained from recordings of producing fragments of DNA by means of gel electrophoresis (data not shown) it can be stated, that the NTCHMTQ at used concentrations did not induce apoptosis after 24, 48 and 72 h exposure and did not influence cell cycle as presented in Figure 4.

On the other hand, the ability of quinazolines to influence cell proliferation and to induce apoptosis was found by many authors [29–35]. The apoptotic fragmentation in cancer cell lines was already reported for quinazolines that are under clinical use in cancer patient [36]: ZD1839 (gefitinib), ZD6474 [37–39], OSI-774 (Tarceva) [40] or are in the preclinical development – doxazosin, HMJ-38 [41, 42], too.

In our previous study, we have shown that NTCHMTQ acted cytotoxically on cell lines L1210 and NIH-3T3 [43]. The sensitivity of leukemia L1210 cells to the quinazoline was higher than that of fibroblast NIH-3T3. The IC_{100} was 12 μM for L1210 cells and 24 μM for NIH-3T3. No effect of quinazoline on the cell cycle profile of L1210 and NIH-3T3 was detected, however quinazoline induced an increase of the sub-G_0 cell fraction, apoptotic DNA fragmentation and apoptotic morphological changes at a concentration of 12 μM. This quinazoline concentration induced caspase 3 activity. Our results demonstrated that induction of apoptotic cell death via activation of caspase 3 contributed to the cytotoxic effects of NTCHMTQ in murine lekemia L1210 cells.

On the other hand, based on our previous study, we have shown that 9-bromo-5-morpholino-tetrazolo[1,5-c]quinazoline (BMTQ) has different effects on the cell cycle of cancer and non cancer cell lines [27]. BMTQ observed the S phase specific effect on the cell cycle of synchronous population of non cancer cell line V79B. In contrast, BMTQ had no effect on the cell cycle profile of asynchronous population of cancer cell lines L1210 and Caco-2 but increased the level of ssDNA breaks in comparison to the control.

The reason why NTCHMTQ induces apoptosis in the L1210 cells via activation of caspase 3 activity however in the B16 cells, which were much more sensitive to NTCHMTQ it induces rather necrosis, is still unclear. It probably depends on a type of a cell line (on the character of the growth of cell line growing in suspension – L1210 cells and of that growing as a monolayer, on a different length of a cell cycle) on the specific drug sensitivity and on the different activation of cell death pathway.

Our results are in accordance with the knowledge that induction of apoptosis by xenobiotics depends on used concentration, time of influence and cell line [44].

Some of quinazolines, such as PD153035 and its N-methyl derivative [45] bind to DNA and behave as typical intercalating agents. In contrast, other quinazolines, such as dialkoxyquinazolines [46] show little interaction with DNA. Therefore in the next part of our study, we monitored possible interaction of quinazoline with dsDNA on electrode surface. DNA-based biosensor acts as an effective chemical toxicity sensor which can be simply used for the rapid detection of DNA damaging species and screening of DNA anticancer compounds. A possibility to investigate redox changes of DNA bases belongs also to advantages of the electrochemical DNA biosensor.

The redox marker can be accumulated effectively within the DNA double helix from the $[Co(phen)_3]^{3+}$ solution at both a polarization of the modified electrode by a positive potential as well as open circuit. Depending on an ionic strength of the medium, intercalation (predominantly at high ionic strength) and electrostatic forces (predominantly at low ionic strength) take part in binding of the marker particles.

DP voltammograms of the $[Co(phen)_3]^{3+}$ indicator at screen-printed electrode after incubation in solution of quinazoline shows no damage to DNA. Little damage was observed by concentration 240 μM. Although some increase in the relative marker signal with decreasing concentration of quinazoline was observed.

In our experiments, we tested the changes of DNA bases. The quinazoline did not cause change of DNA bases. We can say, that the quinazoline can interact by dsDNA intercalation, because NTCHMTQ did not cause damage at the tested concentration. It is the same result, which correlates with results about mutagenity. In our preliminary study concerning the protective effects of [1,2,4]triazolo[4,3-c]quinazolines, we did not found their mutagenic activity on *Euglena gracilic* and NTCHMTQ was very effective DNA protector, particularly at low concentration level, either [47].

Based on results obtained we can conclude that 3-(5-nitro-2-tienyl)-9-chloro-5-morpholine-4-yl[1,2,4]triazolo[4,3-c]quinazoline (NTCHMTQ) manifested the significant *in vitro* cytotoxic/antiproliferative effect. The derivative at cytotoxic concetrations induced morphological changes, the integrity damage of cytoplasmic membrane of HeLa and B16 cell lines and the treated cells were dying by necrosis. On the other hand, at other tested concetrations dose- and time-dependent antiproliferative effects were demonstrated. NTCHMTQ at concentrations tested did not cause changes in cell cycle, did not induce apoptotic cell death in the B16 cells and did not behave as a typical intercalating agent.

Because of the significant *in vitro* antiproliferative effects of NTCHMTQ achieved, the preliminary experiments of antitumor activity *in vivo* on C57BL/6 mice were done. In our preliminary experiments we found out that NTCHMTQ administered intraperitoneally at doses of 1, 10 and 50 mg/kg sligthly reduced the tumor weight. It is known that the effect of the drug depends on an application dose, on the way of application and on dose interval. A route of administration of NTCHMTQ and its effect on anticancer activity will be the object of our next studies.

We would like to thank Dr. HORVÁTHOVÁ for her help measuring cell cycle profiles.

References

[1] WISELOGE FW. Survey of antimalarig drugs 1941–1945. In: Armarego WLF, editor. Advances in heterocyclic chemistry. Vol 1. New York: Academic Press, 1963: 296–304.

[2] ABDEL-RAHMAN TM. Synthesis of some new biologically active 2,3-disubstituted quinazolin-4-ones. Boll Chim Farm 1998; 137: 43–47.

[3] FARGHALY AM, CHAABAN I, KHALIL MA, BEKHIT AA. Non-steroidal antiinflammatory agents. Synthesis of novel 2-pyrazolyl-4(3)-quinazolinones. Arch Pharmacol 1990; 323: 833–836.

[4] POMARNACKA E, ANGIELSKI S, HOPPE A. Derivatives of 4-chloro-5-sulfanoyl-benzoic acid. 8. Synthesis and diuretic activity of pyrazole[3,2-*b*]quinazoline and 1-benzoylpyrazole derivatives. Acta Polon Pharm 1984; 41: 141–151.

[5] KORNET MJ. Synthesis and anticonvulsant activity of 3-alkyl-3,4-dihydro-2(1H)-quinazolinones, J Heterocyclic Chem 1992; 29: 103–105.

[6] SHIMOYAMA M, OGINO K, TANAKA Y, IKEDA T, HISATOME I. Hemodynamic basic for the acute cardiac effects of troglitazone in isolated perfused rat hearts. Diabetes 1999; 3: 609–615.

[7] SORENSON CHM, BARRY MA, EASTMAN A. Analysis of events associated with cell cycle arrest at G2 phase and cell death induced by cisplatin. J Natl Cancer Inst 1990; 82: 749–754.

[8] NAITHANI PK, PALIT G, SRIVASTAVA VK, SHANKER K. 2,3-disubstituted quinazolinones and their antiparkinsonian activity. Ind J Chem Sect B, Org Chem Incl Med Chem 1989; 28: 745–750.

[9] LORIGA M, VITALE G, PAGLIETTI G. Quinoxaline chemistry. Part 9. Quinoxaline analogues of trimetrexate (TMQ) and 10-propargyl-5,8-dideazafolic acid (CB3717) and its precursors. Synthesis and evaluation of in vitro anticancer activity. Farmaco 1998; 53: 139–149.

[10] SOTELO-MUNDO RR, CIESLA J, DZÍK JM, RODE W, MALEY F et al. Crystal structures of rat thymidylate synthase inhibited by Tomudex, a potent anticancer drug. Biochemistry 1990; 38: 087–1094.

[11] JANTOVÁ S, URBANČÍKOVÁ M, MALIAR T, MIKULÁŠOVÁ M, RAUKO P et al. Biological activity of some 4-anilinoquinazolines: cytotoxic, genotoxic and antiprotease effects, induction of necrosis and changes of actin cytoskeleton. Neoplasma 2001; 1: 52–60.

[12] TONKINSON JL, MARDER P, ANDIS SL, SHULTZ RM, GOSSETT LS et al. Cell cycle effects of antifolate antimetabolites: implications for cytotoxicity and cytostatis. Cancer Chemother Pharmacol 1997; 39: 521–531.

[13] RANSON M. Epidermal growth factor receptor tyrosine kinase inhibitors. Br J Cancer 2004; 90: 2250–2255.

[14] POLSHAKOV VI, BIRDSAIL B, FRENKIEL TA, GARGARO AR, FEENEY J. Structure and dynamics in solution of the complex of Lactobacillus casei dihydrofolate reductase with the new lipophilic antifolate drug trimetrexate. Protein Sci 1999; 8: 467–481.

[15] BOS M, MENDELSOHN J, KIM YM, ALBANELL J, FRY DW, BASELGA J. PD153035, a tyrosine kinase inhibitor, prevents epidermal growth factor receptor activation and inhibits growth of cancer cells in a receptor number-dependent manner. Clin Cancer Res 1997; 3: 2099–2106.

[16] YAMAGISHI M, YAMADA Y, OZAKI K, ASA M, SHIMIZU R et al. Biological activities and quantitative structure-activity relationships of spiro[imidazolidine-4-4,-(1H)quinazoline-2,2,5(H)-triones as aldose reductase inhibitors. J Med Chem 1992; 35: 2085–2094.

[17] TAKEMURA Y, JACKMAN A. Folate-based thymidylate synthase inhibitors in cancer chemotherapy. Anti-Cancer Drugs 1997; 8: 3–16.

[18] HAMEL E, LIN CM, PLOWMANl J, WANG HK, LEE KH, PAULL KD. Antitumour 2,3-dihydro-2-(aryl)-4(1H)-quinazolinone derivatives. Interactions with tubulin. Biochem Pharmacol 1996; 51: 53–59.

[19] MODJTAHEDI H, AFFLECK K, STUBBERFIELD C, DEAN C. EGFR blockade by tyrosine kinase inhibitor or monoclonal antibody inhibits growth, directs terminal differentiation and induces apoptosis in the human squamous cell carcinoma HN5. Int J Oncol 1998; 13: 335–342.

[20] HOLDEN SA, TEICHER BA, ROBINSON MF, NORTHEY D, ROSOWSKY A. Antifolates can potentiate topoisomerase II inhibitors in vitro and in vivo. Cancer Chemother 1995; 36: 165–171.

[21] KAYE SB. New antimetabolites in cancer chemotherapy and their clinical impact. Br J Cancer 1998; 78: 1–7.

[22] ŠPIRKOVÁ K, STANKOVSKÝ Š. Amidinoyl isothiocyanates in the synthesis of condensed quinazolines. Preparation of 3-aryl-5,9-disubstituted s-triazolo[4,3-*c*]quinazolines. Collect Czech Chem Commun 1991; 56: 1719–1724.

[23] ŠPIRKOVÁ K, STANKOVSKÝ Š, HORŇÁČEK J. Amidinoyl isothiocyanates in the synthesis of condensed quinazolines. Preparation of 3-aryl-5,9-disubstituted s-triazolo[4,3-*c*]quinazolines and their [1,5-*c*]isomers. Chem Paper 1993; 6: 382–385.

[24] JANTOVÁ S, OVÁDEKOVÁ R, LETAŠIOVÁ S, ŠPIRKOVÁ K, STANKOVSKÝ Š. Antimicrobial activity of some substituted triazoloquinazolines. Folia Microbiol 2005; 50: 90–94.

[25] LABUDA J, BUČKOVÁ M, JANTOVÁ S, ŠTEPÁNEK I, SURUGIU I et al. Modified screen-printed electrodes for the investigation of the interaction of non-electroactive quinazoline derivatives with DNA. J Anal Chem 2000; 367: 364–368.

[26] De-LOS-SANTOS-ALVAREZI P, LOBO-CASTAÑÓN MJ, MIRANDA-ORDIERES J, TUÑÓN-BLANCO P. Electrochemistry of Nucleic Acids at Solid Electrodes and Its Applications. Electroanalysis 2004; 16: 1193–1204.

[27] JANTOVÁ S, THEISZOVÁ M, MIKULÁŠOVÁ M. Cytotoxic and genotoxic effects of some substituted tetrazolo[1,5-c]quinazolines. Neoplasma 2004; 6: 437–442.

[28] JANTOVÁ S, ČIPÁK Ľ, ČERŇÁKOVÁ M, KOŠŤÁLOVÁ D. Effect of berberine on proliferation, cell cycle and apoptosis in HeLa and L1210 cells. J Pharmacol 2003; 55: 1143–1149.

[29] CIARDIELLO F, CAPUTO R, BIANCO R, DAMIANO V, POMATICO G et al. Antitumor effect and potentiation of cytotoxic drugs activity in human cancer cells by ZD-1839 (Iressa), an epidermal growth factor receptor-selective tyrosine kinase inhibitor. Clin Cancer Res 2000; 6: 2053–2063.

[30] FAUST RA, TAWFIC S, DAVIS AT, AHMED K. Apoptosis and growth inhibition of head and neck tumor cell line induced

by epidermal growth factor receptor tyrosine kinase inhibitor. Oral Oncol 1999; 35: 290–295.

[31] KARNES WE JR, WELLER SG, ADJEI PN, KOTTKE TJ, GLENN KS et al. Inhibition of epidermal growth factor receptor kinase induces protease-dependent apoptosis in human colon cancer cell. Gastroenterology 1998; 114: 930–939.

[32] KIMOTO T, HINO K, KOYA-MIYATA S, YAMAMOTO Y, TAKEUCHI M et al. Cell differentiation and apoptosi of monocytic and promyeloytic leukemia cells (U-937 and HL-60) by tryptanthin, an active ingredient of Polygonum tinctorium Lour. Pathol Int 2001; 51: 315–325.

[33] NARLA RK, LIU XP, MYERS DE, UCKUN FM. 4-(3α-bromo-4'hydroxylphenyl)-amino-6,7-dimethoxyquinazoline: a novel quinazoline derivative with potent cytotoxic activity against human glioblastoma cells. Clin Cancer Res 1998; 4: 1405–1414.

[34] PARK JK, LEE SH, KANG JH, NISHIO K, SAIJO N, KUH HJ. Synergistic interaction between gefitinib (Iressa, ZD1839) and oarlitaxel against human gastric carcinoma cells. Anticancer Drugs 2004; 8: 809–818.

[35] SHINTANI S, LI C, MIHARA M, YANO J, TERAKADLO N et al. Gefitinib (Iressa, ZD1839), an epidermal growth factor receptor tyrosine kinase inhibitor, up-regulates p27KIP1 and induces G1 arrest in oral squamous cell carcinoma cell lines. Oral Onco 2004; 1: 43–51.

[36] JAISWAL M, LIPINSKI LJ, BOHR VA, MAZUR SJ. Efficient in vitro repair of 7-hydro-8-oxodeoxyguanosine by human cell extracts: involvement of multiple pathways. Nucleic Acids Res 1998; 26: 2184–2191.

[37] CHANG GC, HSU SL, TSAI JR, LIANG FP, LIN SY et al. Molecular mechanism of ZD1839-induced G1-cell cycle arrest and apoptosis in human lung adenocarcinoma A549 cells. Biochem Pharmacol 2004; 7: 1453–1464.

[38] SANDSTROM M, JOHANSSON M, ANDERSSON U, BERGH A, BERGENHEIM AT, HENRIKSSON R. The tyrosine kinase inhibitor ZD6474 inhibitors tumour growth in an intracerebral rat glioma model. Br J Cancer 2004; 6: 1174–1180.

[39] TRACY S, MUKOHARA T, HANSEN M, MEYERSON M, JOHNSON BE, JANNE PA. Gefitinib induces apoptosis in the EGFR L858R non-small-cell lung cancer cell line H3255. Cancer Res 2004; 20: 7241–7244.

[40] GRUNWALD V, HIDALGO M. Development of the epidermal growth factor receptor inhibitor tarceva (OSI-774). Edv Exp Med Biol 2003; 532: 235–246.

[41] AUSTIN PF, COOK BL, NIEDERHOFF RA, MANSON SR, COPLEN DE WEINTRAUB SJ. Inhibition of mitogenic signaling and induction of apoptosis inhuman bladder smooth muscle cells treated with doxazosin. J Urol 2004; 4: 1662–1665.

[42] YANG Z, BAGHERI-YARMAND R, WANG RA, ADAM L, PAPADIMITRAKOPOULOU VV et al. The epidermal growth factor receptor tyrosine kinase inhibitor ZD1839(Iressa) suppresses c-Src and Pak1 pathways and invasiveness of human cancer cells. Clin Cancer Res 2004; 10: 658–667.

[43] JANTOVÁ S, LETAŠIOVÁ S, REPICKÝ A, OVÁDEKOVÁ R, LAKATOŠ B. The effect of 3-(5-nitro-2-thienyl-9-chloro-5-morpholino-4-yl [1,2,4]triazolo[4, 3-c]quinazoline on cell growth, induction of DNA fragmentation and activity of caspase 3 in murine L1210 cells and fibroblast NIH-3T3 cells. Cell Biochem Funct 2005; 23: in press.

[44] YANG IW, CHOU CC, YUNG BY. Dose-dependent effects of berberine on cell cycle pause and apoptosis in Balb/c 3T3 cells. Naunyn-Schmiedeberg's Arch Pharm 1996; 2: 102–108.

[45] GOOSSENS JF, BOUEY-BENCTEUX E, HOUSSIN R, HENICHART JP, COLSON P et al. DNA interaction of the tyrosine protein kinase inhibitor PD153035 and its N-mathyl analogue. Biochemistry 2001; 15: 4663–4671.

[46] MALECKI N, CARATO P, BENOIT R, GOOSSENS JF, HOUSSIN R et al. Synthesis of condensed quinolines and quinazolines as DNA ligands. Bioorg Med Chem 2004; 12: 641–647.

[47] OVÁDEKOVÁ R, JANTOVÁ S, LABUDA J. Detection of the effective DNA protection by quinazolines using a DNA-based electrochemical biosensor. Analytical Letters 2005; 38: 2625–2638.